Comparisons of Design Methods for Beam String Structure based on Reliability and Progressive Collapse Analysis

Hao Zhou[a], Youbao Jiang[a*], Sondipon Adhikari[b], Qianqian Yin[a], Jianguo Cai [c]

(a School of Civil Engineering, Changsha University of Science and Technology, Changsha 410114, China;

b College of Engineering, Swansea University, Swansea SA1 8EN, United Kingdom;

c National Prestress Engineering Research Center, Southeast University, Nanjing 210096, China)

Abstract: The current design method of ultimate capacity of beam string structure (BSS) is mainly based on the fixed load ratio (FLR) criterion, seldom considers the effect of the random load ratio (RLR) on bearing capacity. In this paper, compared the coefficient of variation (COV) of bearing capacity obtained by RLR criterion with that obtained by FLR criterion. It indicates that the random properties of load ratio have a significant impact on COV and should be accounted for. A more realistic limit state function is built with a practical simplification, which is proved to have a better accuracy by reliability verifications for typical cases. Parametric reliability analyses are also carried out with Monte Carlo simulations. The results show that the reliability with FLR criterion is larger than that with RLR criterion, and thus the reliability of BSS would be overestimated following the current design method and an unsafe design would be resulted in, too. Three targeted reliability indexes are selected to be used for representative cases, and two improved design methods with optimum load and resistance factors are obtained accordingly to minimum the differences between the calculated reliability indexes and targeted ones among cases. Finally, the performance of anti-progressive collapse of BSS designed by the two improved methods is compared when the strut or cable fails. The results show that the representative BSS designed by improved design method 2 with fixed load partial factors and optimum resistance factor which varies with cases has better performance of anti-progressive collapse.

Key words: beam string structure; random load ratio; reliability analysis; load and resistance factors; progressive collapse

Introduction

As a self-balanced system, a beam string structure (BSS) is usually consisting of the upper chord (e g. rigid steel arch), the lower chord (e g. flexible cable), and struts in the middle. In recent years, the BSS has been widely applied in engineering practice due to its light weight, high bearing capacity, good space utilization and beautiful and smooth architectural image (e.g Dong et al. [1]; Zhao et al. [2]; Cai et al. [3]; Luo et al. [4]; Han et al. [5]).

So far, many scholars have carried out works on the structural analysis of BSS. As early as in the 1980s, Satioh et al. [6-8] began to study the basic mechanical principles of the prestressed BSS. Afterwards, Kato et al. [9,10]conducted a theoretical analysis and experimental study on the BSS. To improve the calculation efficiency, many analysis methods for BSS have also been proposed. For example, Thai et al. [11] and Abad et al. [12] proposed new elements for nonlinear finite element analysis of cables under static and dynamic loads, and also presented algorithms for calculating the stiffness matrix and internal force vector; Jiang et al. [13] derived the formulas of geometric nonlinear FEM for spatial beam element, cable element and truss element, respectively. Wu et al. [14,15] investigated the variation of the lateral buckling of the struts in the BSS for different string layouts, and deduced the formulas for calculating the critical buckling load of struts in the BSS. Ye et al. [16] and Cao et al. [17] conducted a study on the structural properties of the beam string structures, and performed numerical simulations and experimental research on the form-finding of beam string structures. Jiang et al. [18] adopted the force method to study the stiffness formulations for cable-arch structures, and proposed an efficient method for stiffness calculation of the concave cable-arch structure. Xue et al. [19,20] used the ANSYS program to perform a design optimization for the BSS of the Shanghai Yuanshen Arena and investigated its bearing capacity through experimental testing.

The wind resistance performance and seismic performance of BSS have attracted significant attentions. Chen et al. [21] studied wind resistance performance of a beam-truss roof structure by means of wind tunnel test, field test and numerical simulation. Han et al. [22] analyzed dynamic stability of beam string structures under earthquake loads, and proposed some suggestions on selecting a proper structural model in project design. Chen et al. [23] studied the dynamic characteristics and wind-induced displacement response of BSS by the finite element method. Lee et al. [24,25] developed a novel two-way beam string structure. The structure is equipped with two types of cables which are arch-shaped and sagging to resist bi-directional loads. Among them, the arched cable mainly resists negative wind pressure.

BSS has been widely used in public buildings because of its strong spanning ability. But compared with the frame structure, the redundancy of BSS is lower, and it is more prone to progressive collapse due to local failures. Therefore, the anti-progressive collapse performance of BSS has been paid more attention by many researchers. Malla et al. [26] analyzed the structural response caused by transient local damage and thought that the risk of collapse of the spatial structure was high. Murtha-Smith et al. [27] analyzed the causes of progressive collapse accidents of a large-span stadium according to the alternate load path method. Hu [28] analyzed the collapse law of BSS under local failure or strong earthquake and put forward the anti-progressive collapse measures that can be applied to design. Cai et al. [29-30] studied the influence of cables or struts failure on BSS based on major engineering projects such as cable-arch structure of the New Guangzhou Railway Station and truss-string structure of the Meijiang Exhibition Center, and proposed some strengthening measures.

Based on the researches above, this structure has been widely used in engineering practices as its design method developed. The conventional design methods mainly follow the FLR criterion, which usually adopt an assumption that ultimate capacity is only affected by the stochasticity of the resistance variables, e.g. steel or concrete strength, section dimensions, neglecting the effects of random properties of load ratio. The structural bearing capacity varies largely with different load ratios (e.g. ultimate capacity of beam string structures under full-span load and half-span load combination, strength of reinforced concrete columns under vertical load and horizontal load combination), and thus the random properties of load ratio have a significant impact on the bearing capacity (see [31-32]). It is reported that the adverse effect on bearing capacity caused by non-uniform snow load may lead to low safety of the BSS designed according to the current load partial factors (see Takahashi et al. [33]).

The previous experimental and theoretical studies mainly focus on the mechanical performance of BSS under the fixed load ratio criterion, while the research on the reliability of BSS under random load ratio is seldom. This paper analyzed the uncertainties of bearing capacity through combining the finite element method with the Monte Carlo simulation, and proposed a simplified approach to establish a more realistic limit state equation of the BSS under both full-span load and half-span load, and carried out the bearing capacity reliability calibration considering the random properties of load ratio. Representative cases are established by selecting three targeted reliability indexes, and the optimum design factors are obtained accordingly to minimum the reliability differences between the calculated reliability and targeted one among cases. The calibration results show that the recommended design factors can achieve the goal better and has better performance of anti-progressive collapse. The results obtained in this paper will enrich the reliability design and Anti-progressive collapse performance of BSS.

Ultimate capacity of BSS with different load ratios

Beam String Structural Analysis Model

In practical engineering problems, two types of BSS, namely, beam string pipeline crossing (BSP, e.g. Shanghai Yuanshen Arena, China) and truss string structure (TSS, e.g. Harbin International Exhibition Center, China) are popular. They differ from the fact that they have different forms of upper chord sections.

For the BSP under the full-span and half-span load combinations, it is assumed that there is sufficient support out of the plane. The basic parameters of the members in this model are shown in Table 1.

Herein, four BSP models with different spans, structural heights and upper chord sections are selected as shown in Table 2.

Table 1 Basic parameters for Members

Members	Section types(mm)	Material strength/MPa	Elasticity modulus /10^5MPa
Upper chord	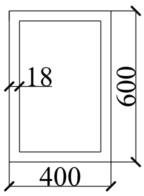	345	2.04

Lower string	163D5	1670	1.90
struts	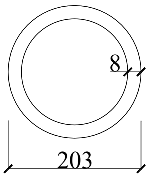	345	2.03

Note: 163D5 means that lower string has 163 wires with diameter 5mm.

Table 2 Four Models of BSP

BSP	Span/m	Structural height/m	Upper chord section/mm
Model 0	63	6.65	600×400×18
Model 1	42	3.36	500×350×12
Model 2	63	7.88	600×400×12
Model 3	77	9.63	700×500×15

For the TSS under the action of full-span and half-span load combination, as shown in Fig. 1, in the same way, it is also assumed that there is sufficient support outside the plane. Jiang et al. [34] reported the basic parameters of this structure. The span is 128m. The rise-to-span ratio of the arch is 0.08, while the sag-to-span ratio of the cable is 0.03. In addition, the steel is considered to be ideal elastic-plastic with yielding strength 345 MPa, and the elastic modulus of the upper chord and struts are 2.0×10^5 MPa. The elastic modulus and prestress of the cables are 1.95×10^5 MPa and 400 MPa, respectively; the spacing between vertical Strut 4 is 9.2m. The sections of all members are shown in Table 3, of which t_1 and t_2 are the thickness of the Chord 1 and Chord 2, respectively. The truss height is 2600mm, and the width between Chord 1 is 3000mm.

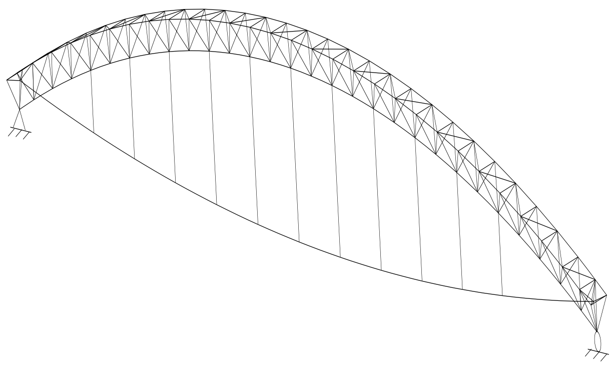

(a)

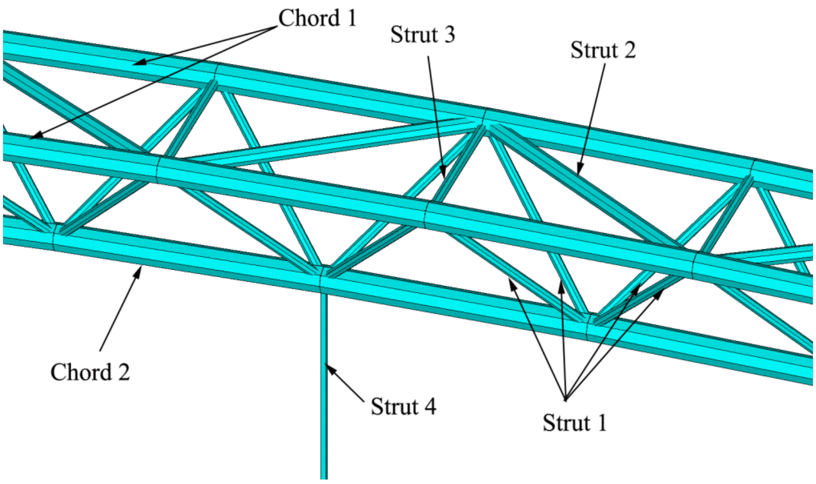

(b)

Fig.1. Model of a TSS:(a)3D view, (b) Truss configurations

Table 3 Sectional dimensions of structure

Member	D/mm	t/mm	Member	Area/mm^2
Chord 1, 2	480	t_1， t_2	Cable	16895
Strut 1	168	6	Strut 3	3051
Strut 2	273	7	Strut 4	7961

Note: *D* refers to the outer diameter of the section, and *t* refers to the section thickness.

Herein, four different schemes of the upper chord section are selected, which nearly has the same steel weight, as shown in Table 4.

Table 4 Four Models of TSS

t/mm	TSS			
	Model 0	Model 1	Model 2	Model 3
t_1	18	16	15	13
t_2	12	16	18	22

Verification of finite element analysis model for BSS

In this paper, the finite element models of BSS are established by ANSYS12.0 software. Geometric nonlinearity and material nonlinearity are considered in the structural analysis. In order to check the finite element models, experimental results are introduced to make comparisons. Taking BSP model as an example, the finite element model of the BSP is shown in Fig. 2, in which the upper chord was simulated by BEAM188 element, and the struts and cables were modeled by LINK8 element and LINK10 element, respectively.

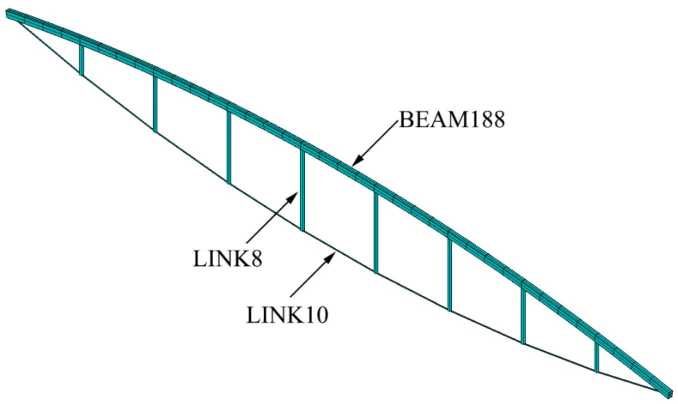

Fig.2. Finite element model of BSP

The test data of mid-span deflection for a scale model of BSP in the literature (the BSS-3 model reported by Xue and Liu [19]) was selected for comparisons, and the results are shown in Fig. 3.

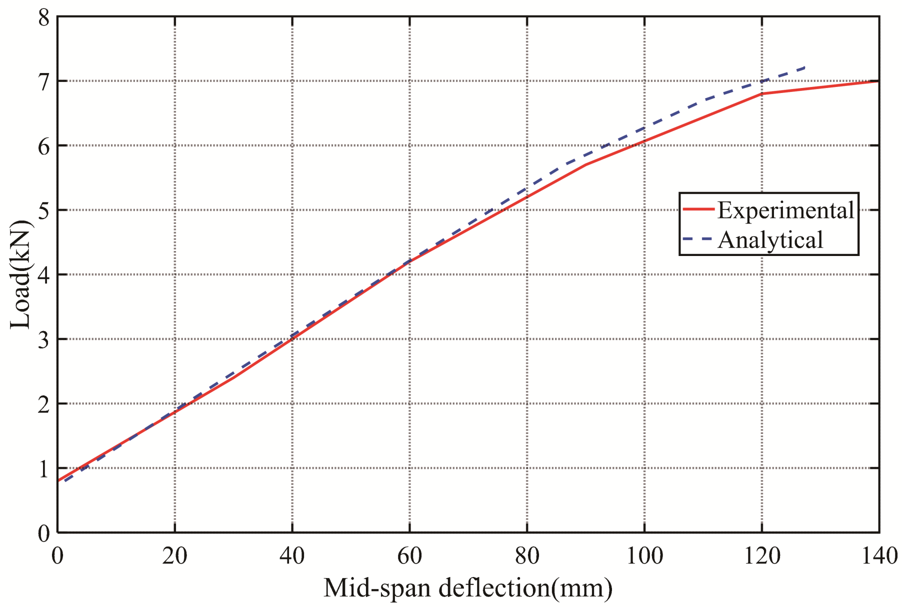

Fig.3. Experimental and analytical mid-span deflections of a BSP model

In Fig. 3, it can be seen that the maximum mid-span deflection of experimental model is about 140mm, while that of analytical model is about 130mm, and the results between two models are close. Moreover, the ultimate bearing capacity of experimental model and analytical model are about 7.0kN and 7.2kN, respectively, and the results between two models are close, too. It shows that the finite element analysis model adopted in this paper has a better accuracy.

Variation of ultimate capacity for BSS with different load ratios

For BSS with full-span load g (e.g. dead load) and half-span load q (e.g. snow load), the ultimate capacity F_u can generally be expressed as the sum of the ultimate loads: g_u and q_u, and is given by:

$$F_u = g_u + q_u \quad (1)$$

Let load ratio be defined as $r=q/g$. Then, taking 8 beam string structure models as examples, the variations of F_u with different values of r are shown in Fig. 4.

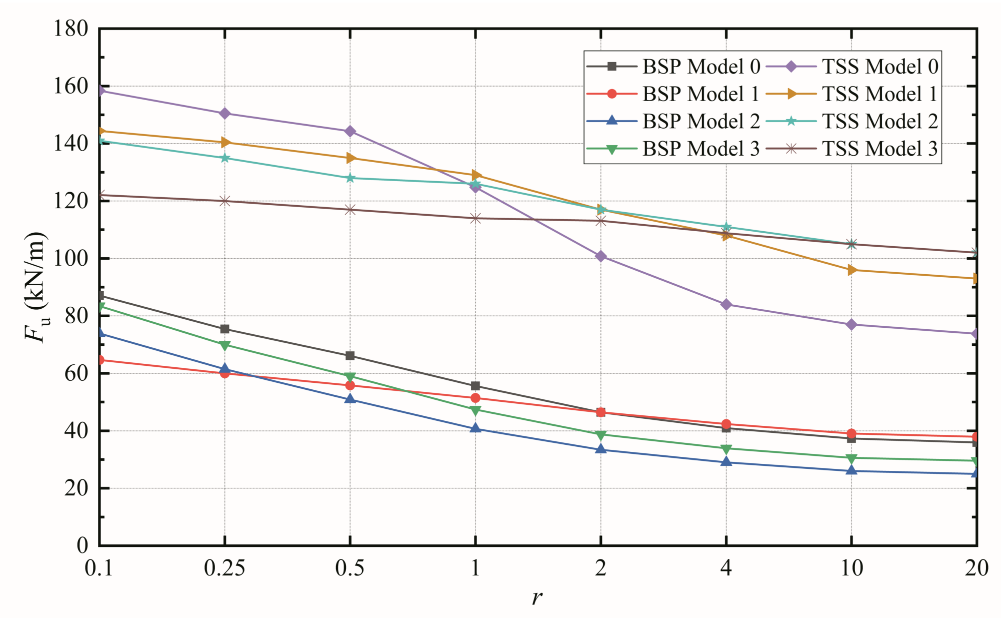

Fig.4. Ultimate capacity of two beam string structures under different load ratios

It can be seen from Fig. 4 that with the increases of load ratio from 0.1 to 20, the ultimate capacities of the BSS models decrease dramatically. For example, the ultimate capacity of TSS Model 0 decreases from 158.4kN/m to 73.8kN/m, by about 53%; while that of BSP Model 2 decreases from 73.92kN/m to 25.03kN/m, by about 66%.

Analysis of ultimate capacity for BSS with random load ratio

Statistics of variables for capacity analysis

As mentioned earlier, the current design method following the FLR criterion. Following this, the load ratio adopts a fixed value. Usually, a nominal load ratio r_n is considered and given by

$$r_\mathrm{n} = q_\mathrm{n} / g_\mathrm{n} \tag{2}$$

where q_n and g_n are nominal values of loads. Actually, the RLR criterion is more realistic due to random properties of load g and load q. Herein, the variation analysis of ultimate capacity is compared for these two cases. Generally, three random variables: load g and q and steel strength f_y, were selected to be considered for their significant effects (see [34]), as shown in Table 5.

Table 5 Distributions of three kinds of random variables

Variable	Distribution	Mean	COV	Reference
g/g_n	Normal	1.06	0.07	[35]
q/q_n	Type I largest	1.14	0.256	[35]
f_y/f_{yn}	Normal	1.09	0.07	[35]

Note: terms with subscript ‘n’ refers to the nominal value of this term.

For FLR case, the finite element analysis results of BSP Model 0 and TSS Model 0 with r_n=0.25, 0.5, 1, and 2, respectively, are obtained by sampling with 1000 runs and shown in Table 6. For typical case r_n=0.25, the frequency histograms of the ultimate capacity for the BSP Model 0 and the TSS Model 0 are shown in Fig. 5 and Fig. 6, respectively.

Table 6 Statistics of ultimate capacity for FLR case

r_n	BSP		TSS	
	mean（kN/m）	COV	mean(kN/m)	COV
0.25	81.48	0.062	147.63	0.063
0.5	70.99	0.066	141.12	0.075
1	60.17	0.068	111.99	0.074
2	50.26	0.064	90.93	0.068

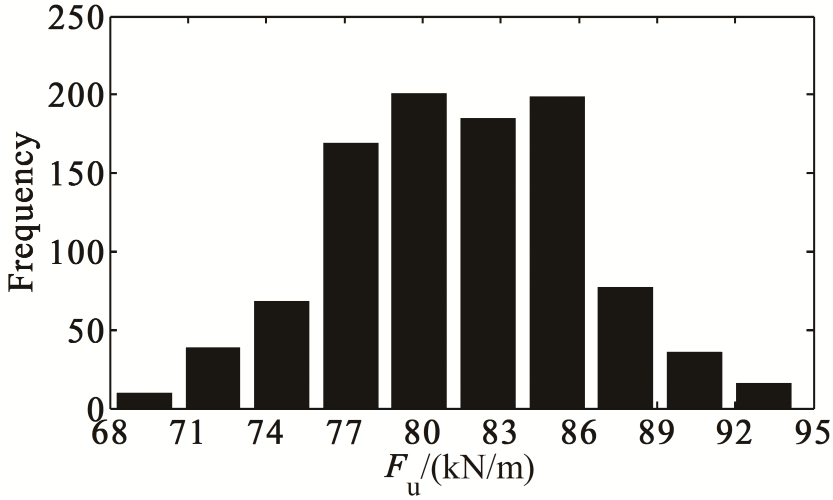

Fig.5. Frequency histogram of ultimate capacity for BSP Model 0 with r_n=0.25

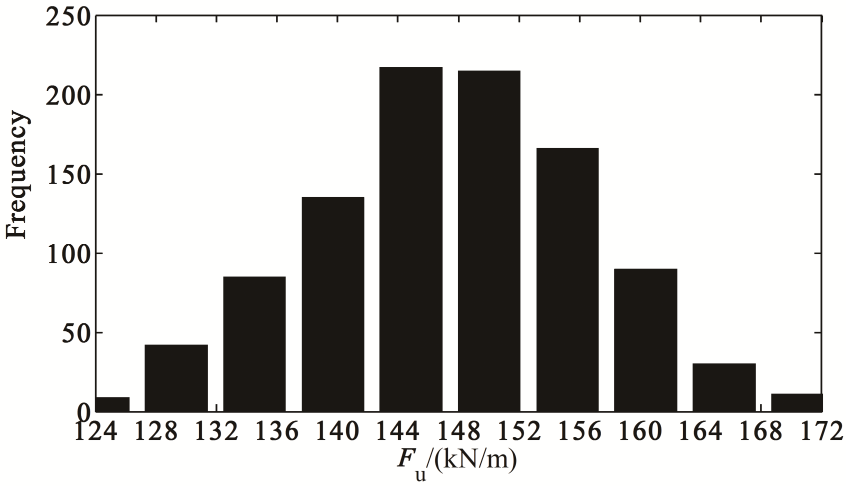

Fig.6. Frequency histogram of ultimate capacity for TSS Model 0 with r_n=0.25

From Table 6, it can be seen that the COV for ultimate capacity of two models is about 0.07, which is close to the statistics of steel strength shown in Table 5. The reason is that only random properties of steel strength is involved in this case.

Table 7 Statistics of ultimate capacity for RLR case

Models	r_n	mean(kN/m)	COV
BSP Model 0	1.0	59.21	0.094
TSS Model 0	1.0	110.38	0.104

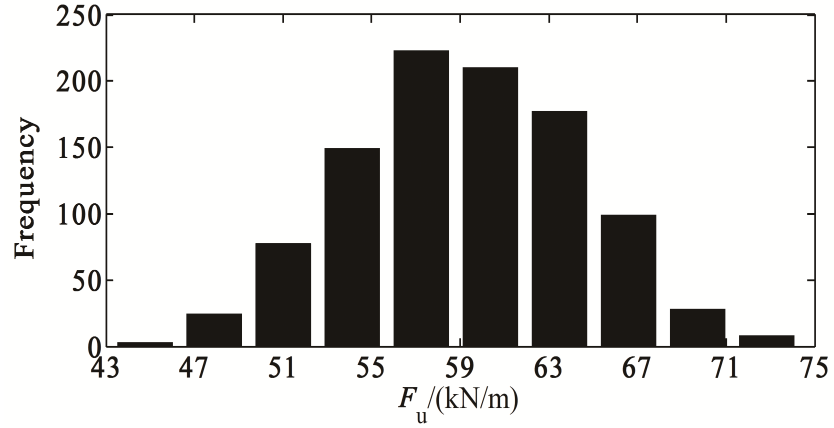

Fig.7. Frequency histogram of ultimate capacity for BSP in RLR case

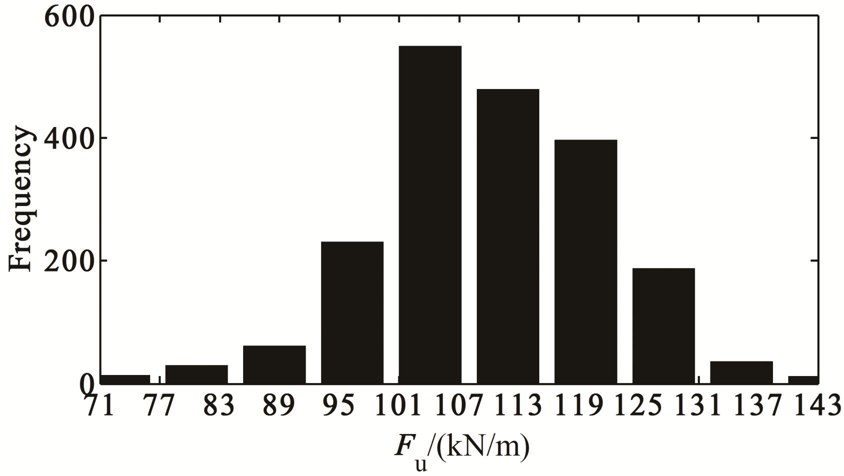

Fig.8. Frequency histogram of ultimate capacity for TSS in RLR case

It can be seen from Table 7 that the COV of ultimate capacity in RLR case is close to 0.1, which is about 42% larger than that in FLR case. Therefore, it can be stated that the randomness of the load ratio has an important influence on the variability of the ultimate capacity for the BSS.

Capacity failure function and reliability analysis of BSS

Simplified capacity model with different load ratio

As early as in 2011, in order to obtain the variation law of capacity under different load ratio, a practical capacity model of some typical structures (e.g. arch structures and beam string structures) under the combination of full-span and half-span load is proposed by Jiang et al. [31], and this model is proved to be well applied through examples verifications. With this model, a relative coefficient of ultimate capacity λ is introduced, and is given by

$$\lambda(r) = \frac{F_{\mathrm{u}}(r)}{F_{\mathrm{u}}(r = 0.1)} = \frac{p_1 r + p_2}{r + p_3} \tag{3}$$

where p_1, p_2 and p_3 are related parameters. If r=∞ (nearly half-span load applied only), λ is close to p_1 in this equation. For this sake, p_1 can be selected to denote the ratio of the capacity with only half-span load to that with r=0.1. For four BSP models and four TSS models above, the values of these parameters are shown in Table 8. The accuracy of model fitting was measured by analyzing the determination coefficient (R^2). Since there is no intercept term in the fitting capacity model, R^2 may be greater than 1. From Table 8, it is seen that the capacity model can be applied well for BSS models. The fitting results of representative models are shown in Fig. 9.

Table 8 Related parameters of capacity model for BSS

Parameters	BSP				TSS			
	Model 0	Model 1	Model 2	Model 3	Model 0	Model 1	Model 2	Model 3
p_1	0.39	0.57	0.32	0.33	0.41	0.60	0.71	0.82
p_2	0.55	0.92	0.43	0.45	1.31	2.19	1.34	2.23
p_3	0.49	0.89	0.36	0.39	1.23	2.15	1.32	2.23
R^2	1.017	0.967	1.018	0.975	0.980	0.994	1.014	1.035

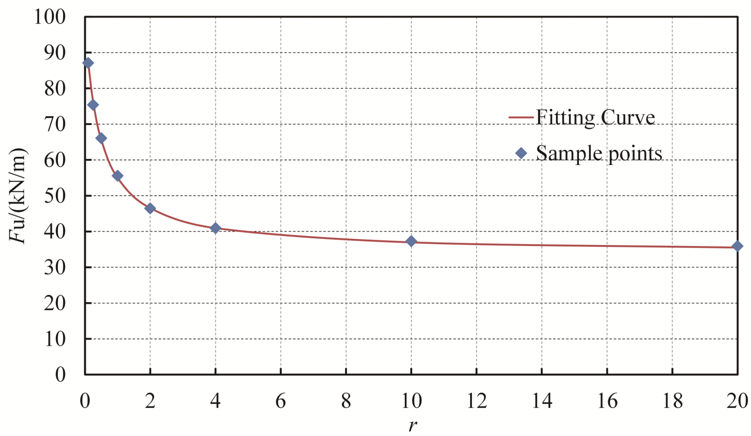

(a) BSP Model 0

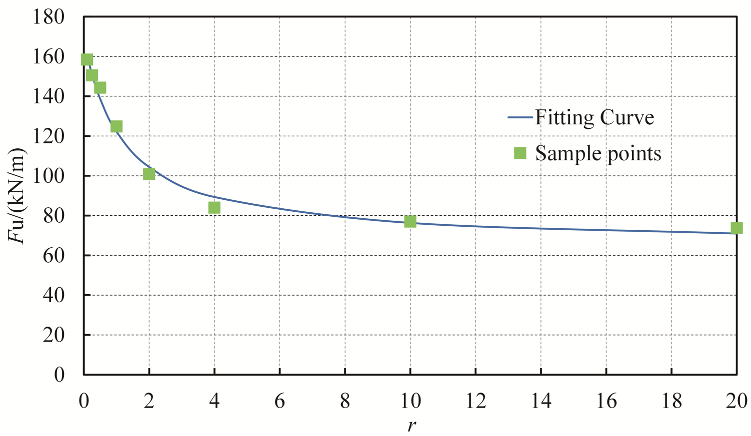

(b) TSS Model 0

Fig.9. Fitting results of representative models

As well known, the ultimate bearing capacity F_{u} is dependent of not only steel strength f_{y} but also load ratio r, thus it is given by

$$F_{\mathrm{u}} = F_{\mathrm{u}}(r, f_{\mathrm{y}}) \tag{4}$$

Then, the more realistic failure function following the RLR criterion is expressed as

$$F_{\mathrm{u}}(r, f_{\mathrm{y}}) - g - q = 0 \tag{5}$$

As mentioned earlier, the current design method for bearing capacity of BSS is mainly based on the FLR criterion. According to this criterion, it is assumed that the load variables does not affect the structural bearing capacity, only the resistance variables (e.g. steel strength) causes the changes of the structural bearing capacity. If F_{u1} is defined as the ultimate capacity under the FLR with r=r_n, which is given by

$$F_{u1} = F_u(r_n, f_y) \tag{6}$$

then the corresponding limit state equation is expressed by

$$F_u(r_n, f_y) - g - q = 0 \tag{7}$$

In Eq. (3), it is assumed that the coefficient of ultimate capacity λ is only dependent of load ratio but independent of steel strength. Based on this assumption, the ultimate capacity satisfies the following equation

$$\frac{F_u(r, f_y)}{F_u(r_n, f_y)} = \frac{\lambda(r)}{\lambda(r_n)} \tag{8}$$

Then, substitute Eq. (8) into Eq. (5), and the limit state equation with RLR is easily built as

$$F_u(r_n, f_y) - (g+q)\frac{\lambda(r_n)}{\lambda(r)} = 0 \tag{9}$$

Comparing Eq. (7) with Eq. (9), it is found that they are largely different and the limit state equation with RLR is more complex.

Uncertainty of resistance calculation model

With regards to a BSS under a given load ratio, the stochastic characteristics of ultimate capacity are related to the uncertainties of steel strength, section dimension and resistance calculation model. Taking into account the small influences of section dimension on reliability due to its small COV (less than 0.05 reported in [35]), its random properties are neglected for simplification. For BSS in engineering practice, cables in BSS are usually designed with high safety level, and upper chord failure usually dominates the significant failure modes. Thus, it can be regarded as a structure with only single steel material for failure uncertainty analysis. Then, the ultimate capacity with FLR for uncertainty analysis is given by

$$F_{\mathrm{u}}(r_{\mathrm{n}}, f_{\mathrm{y}}) = \Omega_{\mathrm{M}} \frac{f_{\mathrm{y}}}{f_{\mathrm{yn}}} F_{\mathrm{u}}^{\mathrm{c}}(r_{\mathrm{n}}, f_{\mathrm{yn}}) \tag{10}$$

where $F_{\mathrm{u}}^{\mathrm{c}}(r_{\mathrm{n}}, f_{\mathrm{yn}})$ is the nominal value of ultimate capacity calculated with the nominal load ratio r_{n} and the nominal strength f_{yn}, and denoted by $F_{\mathrm{un}}^{\mathrm{c}}$ for simplification; Ω_{M} is the model uncertainty of resistance calculation. Then the normalized ultimate capacity is expressed by

$$\frac{F_{\mathrm{u1}}}{F_{\mathrm{un}}^{\mathrm{c}}} = \Omega_{\mathrm{M}} \frac{f_{\mathrm{y}}}{f_{\mathrm{yn}}} \tag{11}$$

If upper chord failure is considered for the structure, which is subjected to bending and compression, then the uncertainty of resistance calculation model of BSS can be selected as that of steel members subjected to bending and compression. Zhang [35] reported that for engineering practices in China, the mean and COV of $f_{\mathrm{y}}/f_{\mathrm{yn}}$ are 1.09 and 0.07, and the mean and COV of Ω_{M} is 1.12 and 0.10, respectively. On the basis of Eq. (10), the mean and COV for the normalized ultimate capacity $F_{\mathrm{u1}}/F_{\mathrm{un}}^{\mathrm{c}}$ can be calculated as $1.09 \times 1.12 \approx 1.22$ and $\sqrt{0.07^2 + 0.10^2} \approx 0.12$, respectively, which is also assumed to be normal variable for simplification.

Reliability analysis of structural ultimate capacity

To satisfy a required target reliability level, the nominal resistance is often determined by magnifying the nominal load effects K times, and is given by

$$F_{\mathrm{un}} = K(g_{\mathrm{n}} + q_{\mathrm{n}}) \tag{12}$$

where K is a safety factor. If load and resistance factors (e.g. dead load partial factor γ_{g}, live load partial factor γ_{q}, resistance partial factor γ_{R}) are used, then Eq. (12) can be rewritten as

$$F_{\mathrm{un}} = \gamma_R(\gamma_g g_{\mathrm{n}} + \gamma_q q_{\mathrm{n}}) \tag{13}$$

In order to verify the accuracy of the simplified method, two typical cases (K=1.7, r_{n}=4.0;

K=2.0, r_n=1.0) are selected to perform reliability analysis with the simplified method and Monte Carlo method (4000; 10000 runs, respectively) for the TSS model 0. Herein, the Monte Carlo method is performed by direct finite element sampling, considering the uncertainty of steel strength f_y, random loads including random ratio r, and resistance calculation model uncertainty Ω_M. The reliability indexes obtained by these two methods are shown in Table 9.

Table 9 Analysis results with two methods for TSS model 0

Two Typical cases	Monte Carlo method		Simplified method	
	β	Time（s）	β	Time（s）
K=1.7, r_n=4.0	2.27	41040	2.08	5
K=2.0, r_n=1.0	2.79	101602	3.05	5

It is seen that the reliability indexes with the simplified method are close to those with the Monte Carlo method, but need much less computational cost. Thus, the simplified method is used to efficiently perform the following parametric reliability analysis.

The reliability indexes of BSP model 0 and TSS model 0 in different cases are shown in Table 10 and Table 11, respectively.

Table 10 Reliability indexes of BSP model 0 under different cases

K	FLR		RLR	
	r_n=1.0	r_n=4.0	r_n=1.0	r_n=4.0
1.7	3.04	2.42	2.49	2.19
1.9	3.40	2.81	2.85	2.55
2.1	3.87	3.13	3.19	2.85

Table 11 Reliability indexes of TSS model 0 under different cases

K	FLR		RLR	
	r_n=1.0	r_n=4.0	r_n=1.0	r_n=4.0
1.7	3.03	2.43	2.51	2.09
1.9	3.49	2.81	2.88	2.42
2.1	3.80	3.13	3.20	2.72

From Table 10 and Table 11, it can be seen that when K and r_n given, the reliability indexes with RLR are all lower than those with FLR. Furthermore, when the load ratio r_n is 4.0, the maximum reliability index with RLR is only about 2.85 (K=2.1, BSP model 0) lower than 3.0. Therefore, in practical engineering, when the half-span load (e.g. snow load) is large, it may lead to an unsafe design, and the structure will possibly collapse. For example, the structure of the roof of the ice-skating rink in Bad Reichenhall, Germany collapsed due to blizzard attack (Dietsch et al. [36]). In addition, Takahashi et al. [33] analyzed the reliability of the steel roof members under snow disaster and found that the reliability level of such members designed according to the Japanese building code is low.

Research on values of design partial factors

Explanations on target reliability indexes

For the target design reliability index of structural member, it is prescribed in Chinese code [37], as shown in Table 12.

Table 12 Target design reliability index of structural member

Failure mode	Safe grade		
	Important	Normal	Not important
Ductile	3.7	3.2	2.7
Brittle	4.2	3.7	3.2

As known, the ultimate capacity of BSS is usually controlled by the upper chord failure, which is flexural-compressive buckling and presents a brittle failure. According to Table 12, the target reliability index can be selected as 3.2, 3.7 and 4.2 for not important, normal, important safe grades, respectively. However, for large load ratio cases (e.g. r_n=4.0), the reliability of BSS models designed by the current design method with K=1.7~2.1 are much lower than the target one, and the reliability differences is large among different cases. Thus, the current design method can not be applied well for different demands and needs to be improved. Herein, based on reliability calibration, two improved methods: improved design 1 and 2 are proposed to try to achieve the goal. The former uses three sets of fixed partial factors for three different safe grades, and the latter uses variable partial factors with cases.

As mentioned earlier, p_1 is a significant parameter. Among the models studied, p_1 is about from 0.32 to 0.82 as shown in Table 8. Herein, 3 representative models are selected as the TSS model 0 (p_1=0.41), the TSS model 3 (p_1=0.82) and the BSP model 2 (p_1=0.32). Moreover, the nominal load ratios are selected as 0.25, 0.5, 1, 2 and 4, respectively. Thus, in the following analysis, 15 structural cases are considered totally.

Optimal partial factors for improved design 1

Generally, the optimal design partial factors are defined as those which can make the design reliability agree with target reliability index well for different cases. To find them, multiple sets of tentative design partial factors are selected for analysis. For each set of design partial factors, the summed reliability error I between design reliability indexes and the target ones can be expressed as:

$$I=\sum_{i=1}^{15}(\beta-[\beta])^2 \tag{14}$$

where $[\beta]$ is the selected target reliability index.

Herein, as many as 180 sets of tentative design partial factors are selected for each target reliability. Through large number of calculations, the results show that the optimal design partial factors for improved method 1 are γ_g=1.15, γ_q=2.3, γ_R=1.15; γ_g=1.15, γ_q=2.1, γ_R=1.40; and γ_g=1.15, γ_q=2.4, γ_R=1.50 for the target reliability indexes 3.2, 3.7 and 4.2, respectively, as shown in Table 13.

Table 13 Optimal design partial factors for three target reliability indexes

$[\beta]$	γ_g	γ_q	γ_R	I_{min}
3.2	1.15	2.3	1.15	0.79
3.7	1.15	2.1	1.4	1.12
4.2	1.15	2.4	1.5	1.2

It is found that the optimum dead load partial factors γ_g are 1.15 for all and these partial factors can achieve the mean reliability close to the target one for the corresponding safe grade (e.g. β_{mean}=3.08 close to $[\beta]$ =3.2 for normal safe grade). To illustrate it clearly, when γ_g=1.15, the variations of the summed reliability error I with different partial factors γ_q and γ_R for all 15 structural cases are shown in Fig. 10. It is seen that the improved design 1 still lead to a large summed reliability error (e.g. larger than 1.2 for $[\beta]$ =4.2 for structural cases)

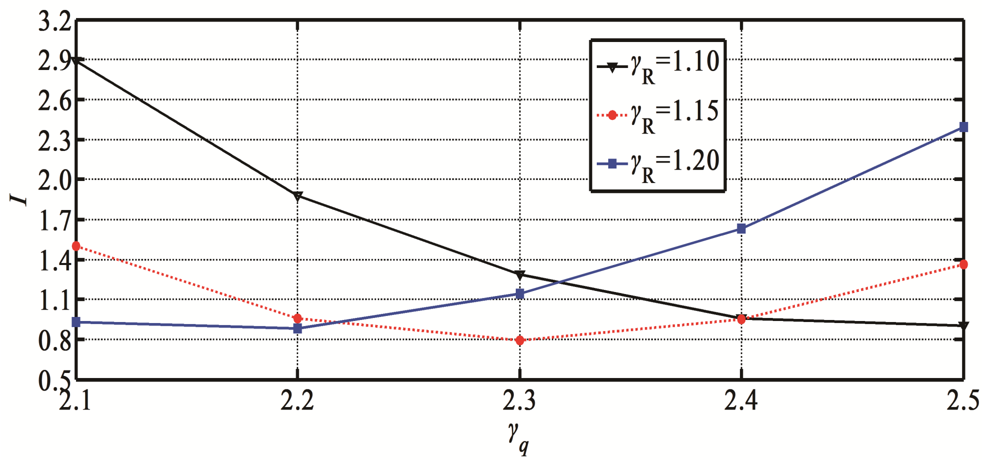

(a) $[\beta]$=3.2

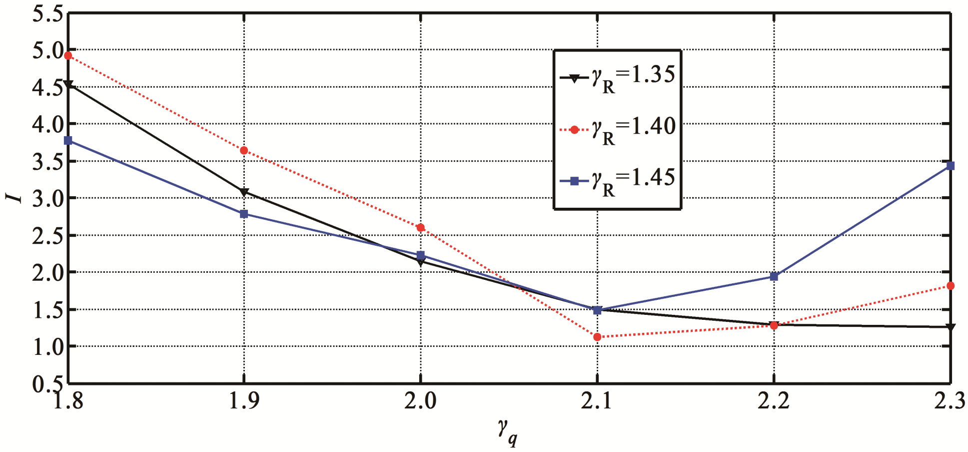

(b) [β]=3.7

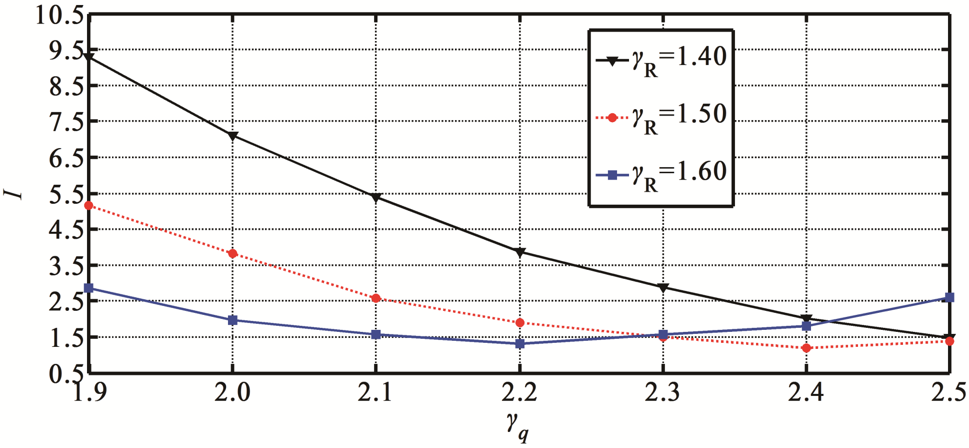

(c) [β]=4.2

Fig.10. Curves of summed reliability error with different design partial factors for BSS

Optimal partial factors for improved design 2

As mentioned earlier, the improved design 1 may result in a large reliability differences among different cases. Thus, the structural design will be unsafe or conservative for cases. To overcome this shortcoming, another method: the improved design 2 is proposed. It uses fixed load partial factors, γ_g=1.15 and γ_q=2.27 (average value of 2.3, 2.1 and 2.4 for 3 safety grades shown in Table 13) and a varing resistance partial factor γ_R. The optimal γ_R is the one with the design reliability closest to the targeted reliability index for total 45 different cases. Based on reliability calibration from case to case, the obtained optimal values of γ_R are shown in Fig. 11.

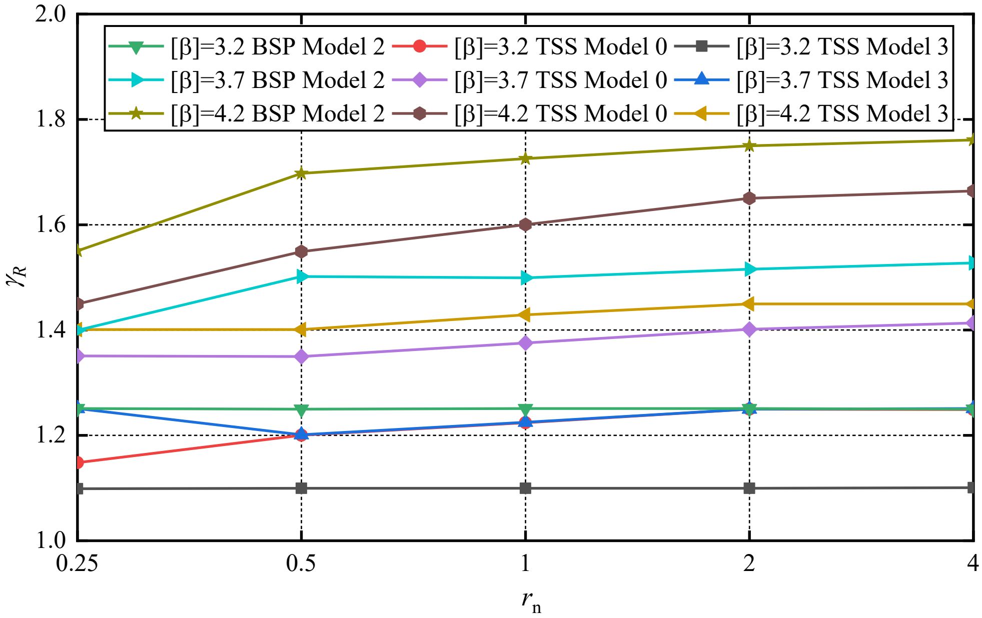

Fig.11. Optimal values of γ_R for different cases

It can be seen from Fig. 11 that the optimal γ_R is not constant, which varies from 1.1 to 1.25 for [β]=3.2 cases, from 1.3 to 1.5 for [β]=3.7 cases and from 1.4 to 1.75 for [β]=4.2 cases, respectively.

Comparisons between different design methods

By comparison, the robustness of the three methods: conventional method (e.g. K=1.9, 2.1), improved method 1, and improved method 2, is evaluated respectively, and the results are shown in Table 14 and Table 15.

Table 14 Robustness evaluation for BSS in conventional method

Conventional Method	β_{max}	β_{mean}	β_{min}	COV
K=1.9	4.20	3.13	2.42	0.18
K=2.1	4.57	3.48	2.72	0.17

Table 15 Robustness evaluation for three target reliability indexes in two methods

Method	[β]=3.2				[β]=3.7				[β]=4.2			
	β_{max}	β_{mean}	β_{min}	COV	β_{max}	β_{mean}	β_{min}	COV	β_{max}	β_{mean}	β_{min}	COV
Improved Method 1	3.69	3.08	2.50	0.09	4.75	3.60	2.34	0.11	5.16	4.02	3.14	0.10
Improved Method 2	3.24	3.20	3.15	0.009	3.76	3.70	3.65	0.01	4.26	4.20	4.14	0.01

It is seen that the average COV with the improved method 2 is the least (about 0.01), which is about 90% lower than that with the improved method 1, and about 95% lower than that with the conventional method. This indicates that the design methods with fixed partial factors (including both the improved design method 1 and the conventional design method) cannot achieve a robust design for the given target reliability level, because the reliability is scattered over a large range among cases. The results also show that the average reliability with the improved method 2 is much closer to the target reliability index value than that with the improved method 1 and the conventional design method. Therefore, the improved method 2 can achieve a more robust reliability design.

Progressive collapse analysis of BSS designed by improved methods

Introduction for progressive collapse analysis

The aforementioned reliability analysis shows that the conventional design method could overestimate the reliability of BSS with random load ratio, resulting in a possible unsafe design, and two improved design methods are proposed to address this phenomenon. It is known that structural progressive collapse has increasingly drawn attentions of researchers and engineers. Herein, a comparison of the improved methods is further analyzed based on the progressive collapse resistance of BSS with local failure. The safety factor should usually be required more than 2.5 for cables according to CECS 212-2006[38], which is much larger than that for other members (e.g., strut) in BSS, therefore it is more likely that the local failure occurred in rigid members or anchor nodes of cable. In this section, taking BSP Model 2 with the target reliability index of 3.7 as an example, the influences of strut failure or anchor failure on the anti-progressive collapse performance are discussed for structures designed by the two improved methods.

At present, there are several methods for simulations of actions of failure member in structural progressive collapse analysis, including static analysis method considering dynamic increment factor, and equivalent load transient unloading method considering initial conditions, and full dynamic equivalent load transient unloading method. It is reported by Zhu et al. [30] that the full dynamic equivalent load transient unloading method could effectively simulate initial conditions under the static load before local member failure, and eliminate the unnecessary dynamic influences of static load on the structure. Herein, this method is also used to perform progressive collapse analysis for BSS with local failure of strut or anchor end of cable. The main steps are as follows:

(1) Carry out a static analysis of the whole structure to extract the internal force P of the local failure member (e.g., strut) under the given load case.

(2) Remove the assumed local failure member as shown in Fig.12(a), and apply the equivalent internal force P as shown in Fig.12(b) to the remaining structure. In t_0 period, the original static load (full-span load and half-span load) and the equivalent load P increase from zero to the maximum; t_1 is the load duration and can be determined by the complete attenuation of forced vibration of the structure under the actions of both original static load and the equivalent load P; T_P is the local member failure stage and taken as 0.00375s (see [39]); T_2 is the attenuation stage when vibration amplitude continuously attenuates under the actions of damping until reaching the final state of stability.

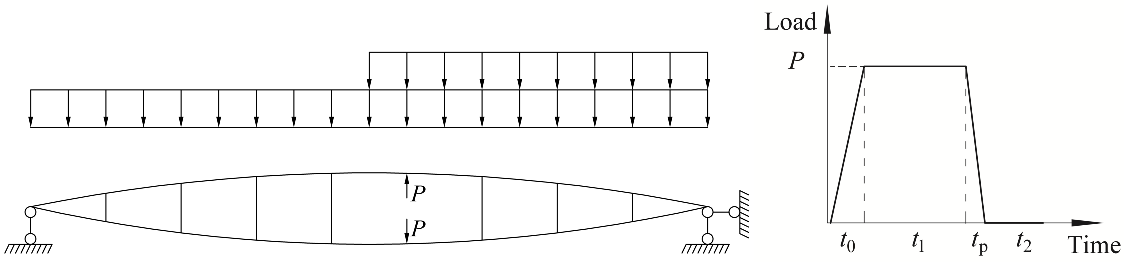

(a) Progressive collapse analysis model of BSS (b) Loading path

Fig.12. The full dynamic equivalent load transient unloading method

FEA modeling of BSS

Based on the techniques on ANSYS/LS-DYNA software in [40], the nonlinear dynamic calculation model with both dynamic and nonlinear effects considered was built for simulation following the alternative load path method. It is known that the structure collapse behavior can be simulated better by the nonlinear dynamic calculation model. The material constitutive model of the upper chord and the strut is ideal elastoplastic model. The cable is composed of high-strength steel wire, with poor ductility, and the failure is characterized by brittle fracture. Therefore, the constitutive model of the cable is assumed to be fracture failure after reaching the ultimate strength, as shown in Fig.13.

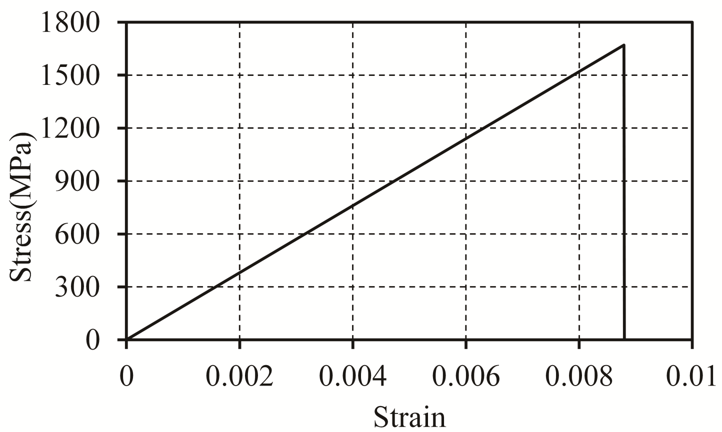

Fig.13. Stress-strain curve of the cable

The collapse of the structure is a transient process, in which the strain rate of steel is very large, so the influence of the material strain rate should be considered in the analysis. The Cowper-Symonds constitutive equation is in good agreement with the experimental data and is widely used. In this paper, the Cowper-Symonds constitutive equation is used to consider the strain rate effect, it can be expressed as:

$$\sigma_{\mathrm{d}} / \sigma_0 = \left[1 + \left(\frac{\varepsilon_{\mathrm{r}}}{C} \right)^{\frac{1}{p}} \right] \tag{15}$$

where σ_d is the dynamic yield stress and σ_0 is the associated static yield stress, ε_r is the strain rate. C and p are strain rate parameter, set as 40.4 and 5.0 respectively (see [41]).

At present, there are many simulations aimed at the anti-progressive collapse of steel structures, but the value of steel failure strain is selected differently. Xie et al. [42] used a failure strain of 3.7% for columns subjected to bending and compression to study the dynamic behavior of steel frames during progressive collapse, and the results are in good agreement with the experimental results. Jiang et al. [43] established a fiber model failure simulation method based on FEMA 356, and stated that when the ultimate strain of the steel is set to 2.5%, the structural responses of failure member during the dynamic process can meet the requirements of the member deformation limit in FEMA 356 well. Tian et al. [44] used the failure strain of 2.5% to simulate the progressive collapse of a large station structure, and stated that when the steel reached this strain value, the structure had excessive deformation and was not conducive to personnel escape and rescue operations. Therefore, the failure strain ε_f of steel is assumed as 0.025 herein for safety reasons. The element would fail if the strain $\varepsilon>\varepsilon_f$, and it is automatically deleted from the FEA model. The automatic single-sided contact ASSC is selected, and the structural damping is assumed as Rayleigh damping with the damping ratio 0.02.

Anti-progressive collapse performance of BSS designed by different methods

Taking the BSP Model 2 with target reliability index 3.7 as an example, the optimum load partial factors and resistance partial factors for the improve method 1 and method 2 are provided in Table 13 and Fig.11, respectively. If two representative load ratios 0.5 and 2.0 are selected, then the corresponding safety factor *K* is calculated with the Eq. (12) and Eq. (13), and the dead load nominal values g_n and the live load nominal values q_n are obtained from the ultimate capacity of BSP Model 2 presented in Fig.4. Finally, these parameters are all shown in Table 16.

Table 16 Parameters of BSS designed by different methods

Design parameters	Improved Method 1		Improved Method 2	
	r_n=0.5	r_n=2.0	r_n=0.5	r_n=2.0
K	2.053	2.497	2.285	2.845
g_n(kN/m)	16.52	4.46	14.85	3.91
q_n(kN/m)	8.26	8.92	7.43	7.82

It can be seen from Table 16 that for the given design method, the safety factor with r_n =2.0 is larger than that when with r_n =0.5; moreover for the given load ratio, the safety factor of improved method 2 is larger than that of improved method 1.

Due to the higher redundancy of the strut, this paper considers the strut failure in two different positions, namely the end Strut 1 and the middle Strut 2. For simplification, they are denoted as ESF (end strut failure) and MSF (middle strut failure) cases, respectively. Herein, the combined load is defined as $1.0g_n+0.5q_n$, and assumed as the equivalent nodal forces acted at the upper chord nodes for analysis. When the BSS which are designed by the two improved methods bear full-span dead load and half-span live load , the overall deformation of the intact structure is S-shaped with upward arch on the left side and concave downward on the right side, as shown in Fig.14.

The sensitivity index of any node in the structure corresponding to the removal of member i can be expressed as:

$$\delta_i=(\Delta-\Delta')/\Delta \tag{16}$$

Where Δ and Δ' are the displacements of the same node of the intact structure and the damaged structure, respectively. When the strut fails, the dynamic response of the maximum upward displacement node and the maximum downward displacement node are extracted, as well as the mid-span node. The node numbers are shown in Fig.15. The calculation results are shown in Table 17-18.

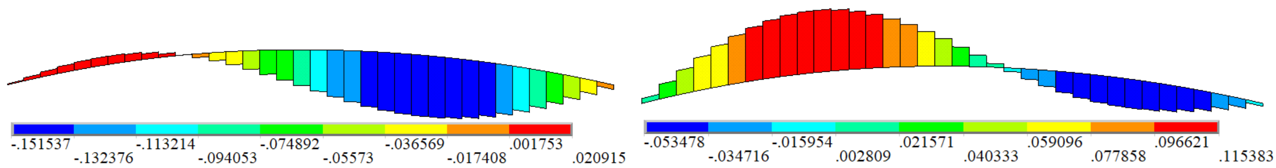

(a) Deflection(m) for r_n=0.5 (b) Deflection(m) for r_n=2.0

Fig.14. Deflections of the upper beam of BSS designed by improved method 1

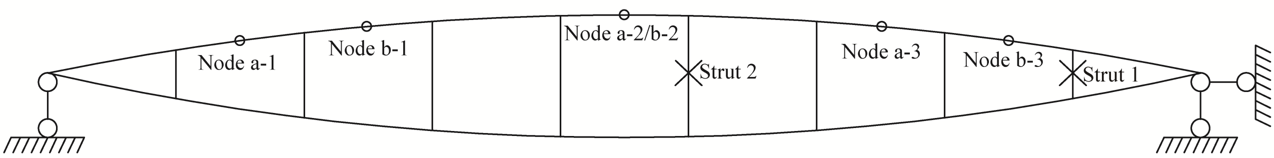

Fig. 15. Failed struts in BSS

Table 17 Node displacement before and after strut failure for Improved Method 1

Node number	r_n=0.5					Node number	r_n=2.0				
	Δ_{intact}	Δ_{ESF}	δ_{ESF}	Δ_{MSF}	δ_{MSF}		Δ_{intact}	Δ_{ESF}	δ_{ESF}	Δ_{MSF}	δ_{MSF}
a-1	0.025	0.014	44%	0.017	32%	b-1	0.120	0.110	8%	0.101	16%

a-2	-0.095	-0.099	-4%	-0.131	-38%	b-2	0.043	0.031	28%	0.016	63%
a-3	-0.148	-0.181	-22%	-0.167	-13%	b-3	-0.048	-0.073	-52%	-0.074	-54%

Table 18 Node displacement before and after strut failure for Improved Method 2

Node	r_n=0.5					Node	r_n=2.0				
number	Δ_{intact}	Δ_{ESF}	δ_{ESF}	Δ_{MSF}	δ_{MSF}	number	Δ_{intact}	Δ_{ESF}	δ_{ESF}	Δ_{MSF}	δ_{MSF}
a-1	0.029	0.009	69%	-0.021	28%	b-1	0.117	0.106	9%	0.094	20%
a-2	-0.074	-0.082	-11%	-0.107	-45%	b-2	0.053	0.039	26%	0.031	42%
a-3	-0.123	-0.153	-24%	-0.141	-15%	b-3	-0.035	-0.060	-71%	-0.058	-66%

When r_n=0.5, due to the failure of Strut 1, the vertical displacement of Node a-3 increases, the vertical displacement of node a-2 changes a little, and the deformation of node a-1 decreases; When r_n=2.0, due to the failure of Strut 1, the vertical displacement of nodes b-2 and b-3 changes greatly, while the change of node b-1 is not significant. The deformation law of BSS after Strut 2 failure is similar to the former, the difference is that the vertical displacement of node a-2 and b-2 changes greatly, the maximum change is 63%. It shows that the local stiffness of the upper chord near the strut decreases due to the failure of a strut, which leads to the increase of local deformation of the upper chord. Under the two improved methods, the deformation law of the structure before and after the strut failure is the same, but the deformation value for the improved method 2 is smaller than that for the improved method 1.

The safety factor of the cable is usually large, but in engineering practices, the cable is still possibly broken due to accidental factors such as material quality defects, maintenance defects, construction defects[45,46]. Moreover, the failure of cable can lead to the overall collapse of BSS. In order to disperse the risk, some researchers propose to split a single cable into multiple cables. For this case, even if one cable fails, the structure can still guarantee the existence of alternative load path [47]. In order to compare the cable safe margin of BSS designed by the two improved methods, assuming that part of the cable at the anchorage end of the cable fails, the critical value of cable area loss leading to BSS collapse is expressed by introducing coefficient ρ, which can be expressed as:

$$\rho = \frac{A_l}{A_i} \tag{17}$$

where A_i is the area of intact cable, A_l is the area of cable loss. The calculation results are shown in Table 19.

Table 19 The critical value ρ of cable area loss leading to the collapse of the BSS

Method	ρ	
	r_n=0.5	r_n=2.0
Improved Method 1	62.80%	81.10%
Improved Method 2	64.50%	82.50%

It is seen that for the BSS designed with the given method, the cable safe margin with r_n=2.0 (e.g. 81.1%) is greater than that with r_n=0.5 (e.g. 62.8%), which is also consistent with the rule of the safety factor in four cases in Table 16. For these two improved methods, the cable safe margin of BSS designed by improved method 2 is greater than that by improved method 1. This indicates that the BSS designed by the improved method 2 shows a better anti-progressive collapse performance than that designed by the improved method 1.

Summary and Conclusions

This paper is aimed at investigating the bearing capacity reliability of beam string structures (BSS) considering the stochastic characteristics of load ratio. The variations of the ultimate capacity for BSS with fixed load ratio and random load ratio are compared and analyzed. A more realistic limit state function based on some simplified ways is established to achieve an efficient analysis of the ultimate capacity reliability of BSS with random load ratio. Finally, the optimal design partial factors are searched accordingly to minimizing the reliability differences between the design reliability and target one, and the performance of anti-progressive collapse of BSS designed by two improved methods is further compared. The main results can be summarized as below:

1） With the increases of load ratio of half-span load to full-span load, the ultimate capacity of BSS decreases dramatically. When the load ratio increases from 0.1 to 20, the ultimate capacity decreases by as much as 66%.

2） The randomness of load ratio has a significant influence on the variability of the ultimate capacity for BSS, and the COV of ultimate capacity for BSS with random load ratio is about from 38% to 65% larger than that with fixed load ratio within the parameters in the analysis.

3） With the simplified capacity model, a more realistic limit state equation can be established and applied efficiently in reliability analysis. The results show that the reliability index with random load ratio criterion is lower than that with the fixed load ratio criterion.

4） The design method with fixed partial factors can lead to large differences between the design reliability and target one among cases, and result in an unsafe design for large load ratio cases for BSS. However, the improved design method with fixed load partial factors and optimum resistance factor which varies with cases can decrease the reliability differences dramatically for different target reliability levels as well as meeting the target reliability indexes well.

5）The representative BSS designed by improved design method 2 with fixed load partial factors and optimum resistance factor which varies with cases has better performance of anti-progressive collapse than that designed by the improved method 1 with fixed partial factors.

The reliability of BSS can be evaluated more reasonably by the method proposed in this paper. To attain a robust design results, it is recommended to select optimum resistance factors according to the actual cases instead of using the fixed resistance factors. Further studies are needed on how to enhance the redundancy of BSS and prevent collapse after local cable failure.

Acknowledgement

The research is supported by the National Natural Science Foundation of China (Grant No. 51678072), the Key Discipline Foundation of Civil Engineering of Changsha University of Science and Technology (18ZDXK01), and the Hunan Provincial Innovation Foundation for Postgraduate (CX20190655). This support is gratefully acknowledged.

References:

[1] Dong SL, Zhao Y, Xing D. Application and development of modern long-span space structures in China[J]. Frontiers of Structural & Civil Engineering, 2012, 6(3):224-239. (DOI: 10.1007/s11709-012-0166-6)

[2] Zhao XZ, Wu A, Xu Z, et al. Research and application of beam string structures[J]. Structural Engineering International, 2015, 25(1):26-33(8). (DOI:10.2749/101686614X14043795570219)

[3] Cai JG, Feng J, Jiang C. Development and analysis of a long-span retractable roof structure[J]. Journal of Constructional Steel Research, 2014, 92(92):175-182. (DOI: 10.1016/ j.jcsr.2013.09.006)

[4] Luo YZ, Li Y, Shen YB, et al.Experimental study on cable-truss reinforced structure system

under heavy load[J]. China Civil Engineering Journal, 2017,50(4):48-56. (in Chinese) (DOI: 10.15951/j.tmgcxb.2017.04.006)

[5] Han Q, Wang L, Xu J. Test and numerical simulation of large angle wedge type of anchorage using transverse enhanced CFRP tendons for beam string structure[J]. Construction & Building Materials, 2017, 144:225-237.(DOI:10.1016/j.conbuildmat.2017.03.150)

[6] Saitoh M, Kuroki F. Structural planning of beam string structure [C]. Space Structures for Sports Buildings-Proceedings of the International Colloquium on Space Structures for Sports Buildings, 1987, 1995:693-694.

[7] Saitoh M, Nakakawaji I. A Study on structural characteristic of beam string structure : Part 1 Prestressing for Dead Load[C]//. Summaries of Technical Papers of Meeting Architectural Institute of Japan. Architectural Institute of Japan, 1987.

[8] Saitoh M, Okada A. The role of string in hybrid string structure[J]. Engineering Structures, 1999, 21(8):756-769. (DOI:10.1016/S0141-0296(98)00029-7)

[9] Kato S, Nakazawa S, Matsue Y, et al. Active control of axial forces in beam string space frames [C]//.IASS-ASCE International Symposium, 1994:664-673.

[10] Kato S , Nakazawa S , Okada Y . optimum locations for actuators to reduce the responses of beam string struc structures to static and dynamic disturbance [C]// Asia-pacific Conference on Shell & Spatial Structures, 1996:688-695.

[11] Thai H T, Kim S E. Nonlinear static and dynamic analysis of cable structures[J]. Finite Elements in Analysis & Design, 2011; 47(3):237-246. (DOI:10.1016/j.finel.2010.10.005)

[12] Abad M S A, Shooshtari A, Esmaeili V, et al. Nonlinear analysis of cable structures under general loadings[J]. Finite Elements in Analysis & Design, 2013; 73(73):11-19. (DOI:

10.1016/j.finel.2013.05.002)

[13] Jiang ZR, Xu M, Duan WN, et al. Nonlinear Finite Element Analysis of Beam String Structure[J]. Advanced Materials Research, 2011, 163-167:2124-2130. (DOI: 10.4028/ www.scientific.net/amr.163-167.2124)

[14] Wu M. Analytical method for the lateral buckling of the struts in beam string structures[J]. Engineering Structures, 2008; 30(9):2301-2310. (DOI:10.1016/j.engstruct.2008.01.008)

[15] Wu M, Hirai K. Lateral buckling of the struts in beam string structures considering the layout of strings [J]. International Journal of Structural Stability & Dynamics, 2012, 12(03):1250015. (DOI:10.1142/S0219455412500150)

[16] Ye J, Feng R Q, Liu B. A form-finding method of beam string structures — Offload by steps method[J]. International Journal of Steel Structures, 2012, 12(2):267-283. (DOI: 10.1007/ s13296-012-2010-1)

[17] Cao ZG, Feng BS. Form finding analysis of large-span spindle Tensairity beam[J]. Journal of Harbin Institute of Technology, 2016, 48(06): 25-29 (in Chinese) (DOI: 10.11918 /j.issn. 0367-6234. 2016. 06. 004)

[18] Jiang YB, Cao Q, K X, et al. Stiffness study of inner concave cable–arch structure based on an efficient method. Advances in Structural Engineering, 2016; 19(12):1927-1939. (DOI: 10.1177/1369433216649394)

[19] Xue WC, Liu S. Design optimization and experimental study on beam string structures[J]. Journal of Constructional Steel Research, 2009; 65(1):70-80. (DOI: 10.1016/j.jcsr.2008.08.009)

[20] Xue WC, Liu S. Studies on a Large-Span Beam String Pipeline Crossing[J]. Journal of Structural Engineering, 2008; 134(10):1657-1667. (DOI: 10.1061/(ASCE)0733-9445(2008)

134:10(1657))

[21]Chen FB, Li QS, Wu JR, et al. Wind effects on a long-span beam string roof structure: Wind tunnel test, field measurement and numerical analysis[J]. Journal of Constructional Steel Research, 2011; 67(10):1591-1604. (DOI: 10.1016/j.jcsr.2011.04.003)

[22] Han QH, Ma CY, Zhang JY. Dynamic stability analysis of beam string structures under earthquake loads[J]. Advanced Steel Construction, 2007, 3(3): 679-688. (DOI:10.1016/ B978-008044637-0/50179-7)

[23] Chen YJ, Feng ZF, Qi A, et al. The analysis of dynamic characteristics and wind-induced displacement response of space Beam String Structure[C], 2018 4^{th} International Conference on Energy Materials and Environment Engineering (ICEMEE 2018), 2018,38: 03032.

[24] Lee S , Seo M , Baek K Y , et al. Experimental study of two-way beam string structures[J]. Engineering Structures, 2019, 191:563-574. (DOI.org/10.1016/j.engstruct.2019.04.033)

[25] Lee S , Seo M , Park S , et al. Geometrical Parametric Study on Two-Way Beam String Structures[J]. Journal of the Korean Association for Spatial Structures, 2019, 19(3):69-76. (DOI.org/10.9712/KASS.2019.19.3.69)

[26] Malla R B , Nalluri B B. Dynamic effects of member failure on response of truss-type space structures[J]. Journal of Spacecraft & Rockets,1995, 32(3):545-551. (DOI:10.2514/3.26649)

[27] Murtha-Smith E A. Alternate path analysis of space trusses for progressive collapse [J]. Journal of Structural Engineering, ASCE, 1988, 114 (9):1978-1999. (DOI: 10.1061 /(ASCE) 0733- 9445 (1988)114:9(1978))

[28] Hu SL. Progressive collapse analysis and anti-collapse design of beam string structure[D]. Beijing: Beijing University of Technology,2010: 1-154. (in Chinese)

[29] Cai JG, Wang FL, Feng J, et al. Progressive collapse analysis of cable-arch structures of the New Guangzhou Railway Station [J]. Journal of Building Structures, 2010, 31(7):103-109. (in Chinese) (DOI:10.14006/j.jzjgxb.2010.07.013)

[30] Zhu YF, Feng J, Cai JG, et al. Analysis on progressive collapse resistance of truss string structure of Meijiang Exhibition Center [J]. Journal of Building Structures, 2013, 34(3):45-53. (in Chinese) (DOI:10.14006/j.jzjgxb.2013.03.003)

[31] Jiang YB, He YH. Research on load effect function model under full-span and half-span loading [J]. Engineering Mechanics 2011; 28(2):123-128. (in Chinese)

[32] Jiang YB, Zhou H, Michael Beer, etc. Robustness of Load and Resistance Design Factors for RC Columns with Wind-Dominated Combination Considering Random Eccentricity[J]. Journal of Structural Engineering 2017; 143(4):1-9. (DOI:10.1061/(ASCE)ST.1943-541X.0001720.)

[33] Takahashi T, Ellingwood B R. Reliability-based assessment of roofs in Japan subjected to extreme snows: incorporation of site-specific data[J]. Engineering Structures 2005; 27(1):89-95. (DOI:10.1016/j.engstruct.2004.09.001)

[34] Jiang YB, Zhou CY, Zhou H. Robustness of ultimate capacity for arch truss string structure with random ratio of half-span load to full-span load[C]. 6th Asian-Pacific Symposium on Structural reliability and its applications, 2016, Shanghai, China.

[35] Zhang XP. Reliability analysis and design for building structures [M]. Beijing: Science Press; 2001:1-107. (in Chinese)

[36] Dietsch P , Winter S . Structural failure in large-span timber structures: A comprehensive analysis of 230 cases[J]. Structural Safety, 2018, 71:41–46. (DOI: 10.1016/j.strusafe.2017.11. 004)

[37] GB50068-2001 Unified standard for reliability design of building structures，Beijing，China，Architecture & Building press.(in Chinese)

[38]CECS 212-2006《Technical specification for prestressed steel structures》，Beijing， China，China Planning Press.(in Chinese)

[39]Mozos C M , Aparicio A C. Numerical and experimental study on the interaction cable structure during the failure of a stay in a cable stayed bridge[J]. Engineering Structures, 2011, 33(8):2330-2341. (DOI:10.1016/j.engstruct.2011.04.006)

[40]LS-DYNA® Keyword User's Manual Volumn II: Material Models[M]. California: Livermore Software Technology Corporation, 2013.

[41] Lu Y, Liu K, Wang ZL, Tang WY. Dynamic behavior of scaled tubular K-joints subjected to impact loads[J]. Marine Structures, 69 (2020) 102685. (DOI: org/10.1016/j.marstruc.2019. 102685)

[42] Xie FZ , Gu B , Qian H . Experimental study on the dynamic behavior of steel frames during progressive collapse - ScienceDirect[J]. Journal of Constructional Steel Research, 2021, 177: 106459. (doi.org/10.1016/j.jcsr.2020.106459)

[43]Jiang L，Ni JG，Qu G, et al. Study on key issues of progressive collapse resistance capacity analysis for complex high-rise steel structure[J]. Journal of Building Structures, 2019, 40(6): 155-165. (in Chinese) (DOI: 10.14006/j.jzjgxb.2018.c299)

[44]Tian CH, Dong C, Liu M, et al. Simulation analysis of progressive collapse for a station[J]. Journal of Railway Engineering Society, 2015, 32(12) :76-79. (in Chinese)

[45]Shoghijavan M, Starossek U. An analytical study on the bending moment acting on the girder of a long-span cable-supported bridge suffering from cable failure [J]. Engineering Structures,

2018, 167: 166 − 174. (DOI: 10.1016/j.engstruct.2018.04.017)

[46]Guo J, Zhou G, Zhou D, et al. Cable fracture simulation and experiment of a negative Gaussian curvature cable dome [J]. Aerospace Science and Technology, 2018, 78: 342 − 353. (DOI: 10.1016/j.ast.2018.04.033)

[47] Liu GG, Wu ZW, Cai J. Study on static and dynamic behaviors of truss string structure with double cables[C]//Proceedings of Seventh International Conference on Advances in Steel Structure, 2012: 900-907.